

## Original Article

---

### Informatics Center for Mouse Genomics

#### *The Dissection of Complex Traits of the Nervous System*

Glenn D. Rosen,<sup>\*,1</sup> Nathan T. La Porte,<sup>1</sup> Boris Diechtiareff,<sup>1</sup> Christopher J. Pung,<sup>1</sup> Jonathan Nissanov,<sup>2</sup> Carl Gustafson,<sup>2</sup> Louise Bertrand,<sup>2</sup> Smadar Gefen,<sup>2</sup> Yingli Fan,<sup>2</sup> Oleh J. Tretiak,<sup>3</sup> Kenneth F. Manly,<sup>4</sup> Melburn R. Park,<sup>5</sup> Alexander G. Williams,<sup>5</sup> Michael T. Connolly,<sup>5</sup> John A. Capra,<sup>5</sup> and Robert W. Williams<sup>5,6</sup>

<sup>1</sup>Department of Neurology, Division of Behavioral Neurology, Beth Israel Deaconess Medical Center and Harvard Medical School, Boston, MA 02215; <sup>2</sup>Departments of Neurobiology & Anatomy, Drexel College of Medicine, <sup>3</sup>Electrical and Computer Engineering, Drexel University, Philadelphia, PA 19104; <sup>4</sup>Molecular & Cellular Biology, Roswell Park Cancer Institute, Buffalo, NY 14263; <sup>5</sup>Department of Anatomy and Neurobiology, <sup>6</sup>Center of Genomics and Bioinformatics, University of Tennessee Health Science Center, Memphis TN 38163

#### **Abstract**

In recent years, there has been an explosion in the number of tools and techniques available to researchers interested in exploring the genetic basis of all aspects of central nervous system (CNS) development and function. Here, we exploit a powerful new reductionist approach to explore the genetic basis of the very significant structural and molecular differences between the brains of different strains of mice, called either complex trait or quantitative trait loci (QTL) analysis. Our specific focus has been to provide universal access over the web to tools for the genetic dissection of complex traits of the CNS—tools that allow researchers to map genes that modulate phenotypes at a variety of levels

ranging from the molecular all the way to the anatomy of the entire brain.

Our website, The Mouse Brain Library (MBL; <http://mbl.org>) is comprised of four interrelated components that are designed to support this goal: The Brain Library, iScope, Neurocartographer, and WebQTL. The centerpiece of the MBL is an image database of histologically prepared museum-quality slides representing nearly 2000 mice from over 120 strains—a library suitable for stereologic analysis of regional volume. The iScope provides fast access to the entire slide collection using streaming video technology, enabling neuroscientists to acquire high-magnification images of any CNS region for any of the mice in the MBL.

\*Address to which all correspondence and reprint requests should be sent.

E-mail: [grosen@bidmc.harvard.edu](mailto:grosen@bidmc.harvard.edu)

Neurocartographer provides automatic segmentation of images from the MBL by warping precisely delineated boundaries from a 3D atlas of the mouse brain. Finally, WebQTL provides statistical and graphical analysis of linkage between phenotypes and genotypes.

**Index Entries:** Brainspatial normalization; brain atlas; histology; stereology; video microscopy; QTL; neurogenetics; genetics; mouse.

### Complex Trait Analysis: The Beauty of Variability

The project described here grew out of our mutual interest in the dissection of the complex network of molecules and mechanisms that modulate growth of different parts of the brain. Specifically, we are concerned with mapping the genes that modulate complex neuroanatomic traits. These quantitative phenotypic traits can be measured at a variety of levels, ranging from gross size of specific structures (e.g., hippocampus, striatum), to the number of neurons and neuronal subtypes contained within these regions, to the expression levels of specific genes. To do this, we have leveraged the explosive growth in tools and techniques in the fields of stereology, genetics, and bioinformatics to create an integrative approach to this problem. Toward that end, we have assembled the analytic tools, tissue resources, and genotypes essential for systematic exploration of the complex genetics of mammalian brain architecture. This quantitative genetic approach highlights sets of normally variable genes—quantitative trait loci (QTLs)—that contribute to differences in the size, shape, and architecture of the brain and also control cell proliferation and cell survival in the central nervous system (CNS).

The key to QTL (alternately called “complex trait”) analysis is the exploitation of the wide range of normal variation for a given phenotype. In our particular case, it is fortuitous that

normal variation of the CNS can be impressive. Numbers of neurons in the human neocortex vary from 15 to 32 billion (Pakkenberg and Gundersen, 1997). The volume and cell number of the human visual cortex vary threefold, as does the density of cones in the foveal pit (Stensaas et al., 1974; Curcio and Allen, 1990; Gilissen and Zilles, 1996; Gilissen and Williams, 1997). Numbers of ocular dominance columns within the primary visual cortex of rhesus monkeys vary by more than 50% (Horton and Hocking, 1996). These robust differences are caused not by mutations but by the cumulative action of many normally variable genes and by the action of numerous developmental and environmental factors. Normal genetic polymorphisms are the most critical source of variance: they are the substrate for evolutionary and developmental modification of brain size and cellular architecture (Williams and Herrup, 1988; Lipp et al., 1989; Williams et al., 1993).

It is the case, however, that we remain quite ignorant about normal variation in CNS structure in mice. Why is this so? The main reasons have to do with the research strategies of most neuroscientists. First, most investigators would rather study extreme phenotypes—the striking mutations, knockouts, and transgenic mice that grace the covers of *Cell*, *Science*, and *Neuron*. The larger the effect of a mutant or null allele is, the easier the analysis of the controlling molecular and cell biological process. Second, many neuroscientists tend to regard variation as an experimental nuisance to be minimized or eliminated before they try to expose fundamental mechanisms of brain development, structure, and behavior. They are attracted to the study of mice precisely because it is possible to order large numbers of genetically identical animals.

In contrast, we embrace the normal variation seen between strains of isogenic mice. Although mutants and knockouts most assuredly are useful, we require more generic

methods that can target any and all CNS regions and cell types. Thus, instead of depending on rare mutations and knockouts, we exploit methods that provide information about common gene variants—the normal gene polymorphisms that are responsible for the far more pervasive and important natural variation found within typical populations of animals. Complex trait analysis, the approach we describe here, was developed rapidly in the late 1990s as a result of the hybridization of quantitative genetics and molecular genetics (Lander and Schork, 1994). The suite of techniques associated with this approach has greatly extended the variety of CNS phenotypes that can be subjected to systematic molecular analysis. In neuroscience, complex trait analysis has been embraced by behavioral geneticists and neuropharmacologists (Plomin et al., 1991; Johnson et al., 1992; Crabbe et al., 1994; Takahashi et al., 1994; Kanets et al., 1996). In our own laboratories, we have used complex trait analysis to map QTLs associated with a variety of neuroanatomic phenotypes, including retinal ganglion cell (Williams et al., 1996; Williams et al., 1998) and striatal neuron number (Rosen and Williams, 2001), the weight of the whole brain (Williams, 2000), hippocampus (Lu et al., 2001), cerebellum (Airey et al., 2001) and olfactory bulbs (Williams et al., 2001b), the volume of the striatum (Rosen and Williams, 2001) and cerebellum (Airey et al., 2001), and cerebral ventricle size (Zygourakis and Rosen, 2003). Using the tools described in the following, we aim to provide online access for laboratories worldwide to gather neuroanatomic phenotypes at a variety of levels and relate these to modulating genes.

### **Informatics Center for Mouse Neurogenetics**

The specific objective of our collaboration is to perform a systematic and highly detailed genetic dissection of the mouse brain by assem-

bling and exploiting a suite of image databases, motorized video microscopes, and software to explore the genetic basis of structural and morphometric variation of the mouse CNS. The mouse is the ideal mammal to exploit in developing these neurogenetic resources. There are hundreds of isogenic strains of mice that have been behaviorally phenotyped and are genetically well-characterized. Combining these genetic and phenotypic databases with those generated by neuroanatomic investigations will provide a powerful tool for broader understanding of the genetic modulation of brain and behavior. Our resources are open to the entire research community for collaborative and independent analysis over the Internet. It is our goal to catalyze far more extensive research on the quantitative genetics of CNS structure in mice, and ultimately in humans, than any single group would ever be able to handle.

Our collaborative project is comprised of four components, each of which will be discussed below. The centerpiece of our project is The Mouse Brain Library (MBL)—an ever-expanding image database of museum-quality histologically prepared slides that are suitable for stereologic analysis of regional volume. The iScope provides fast access to the entire slide collection using streaming video technology, enabling neuroscientists to acquire high-magnification images of any CNS region for any of the mice in the MBL. Neurocartographer provides automatic segmentation of images from the MBL by warping precisely delineated boundaries from a 3D atlas of the mouse brain. Finally, WebQTL provides statistical and graphical analysis of linkage between phenotypes and genotypes.

### **The Mouse Brain Library ([mbl.org](http://mbl.org))**

The MBL houses an expanding collection of high-resolution images of histological slides taken from nearly 2000 mice representing over 120 different genetically distinct strains. Each



Fig. 1. Dynamic imaging of histologic slides over the web. Slides from the MBL can be dynamically imaged at various resolutions. The panel on the left shows a full slide, and the panel in the middle is the result of zooming in on one section of interest. The rightmost panel is represents the highest resolution ( $4 \mu\text{m}/\text{pixel}$ ) of these images.

slide contains a 1-in-10 (every 10th section) systematic sample of sections throughout an individual mouse brain and each brain is represented by two slides separated by five sections. These sections are cut in the coronal or horizontal plane, and are dynamically presented at a variety of resolutions. Each slide is imaged at a maximal resolution of  $4 \mu\text{m}/\text{pixel}$  using Virtual Slice (Microbrightfield), which creates an  $18,400 \times 12,750$  pixel image using  $2.4 \times$  microscopic magnification. Users can interactively pan and zoom these images using the free Flash plug-in (Macromedia Inc.), and they can download any portion of the image at a variety of resolutions (Fig. 1).

These images can subsequently be imported into image analysis programs (i.e., Image/J or NIH Image) where volumes can be stereologically determined. They are also used in the navigational windows of the iScope interface described later. In the future, we hope to integrate similar image analysis tools into the web site directly. In addition to these images, the MBL contains atlases, magnetic resonance images (MRIs), and databases containing neuroanatomic and genetic information.

The images themselves are obviously essential to the aim of providing users with the ability to quantitatively measure neuroanatomic features, but the goal of furnishing the tools for complex trait analysis is only as strong as the underlying genetic information. In that vein, the lynchpin of the MBL itself lies in the choice of isogenic strains, specifically with our emphasis on gathering a complete collection of brains from a variety of recombinant inbred (RI) strains. RI strains are isogenic strains of mice that have derived from common parental stock. Thus each "line" of an RI "set" shares alleles, but over generations of inbreeding, they have recombined in such a way that the alleles are assorted differentially between the lines (Fig. 2).

RI strains have been used for several decades to map complex polygenic traits by statistically aligning the phenotypic differences between the strains with the known genetic differences between these strains with the measured phenotypes. The MBL contains up-to-date genetic information for each of the RI lines in the image database, and WebQTL (*see also* Wang et al., this issue) provides the tools to map neuroanatomic (or any other) phenotypic trait.

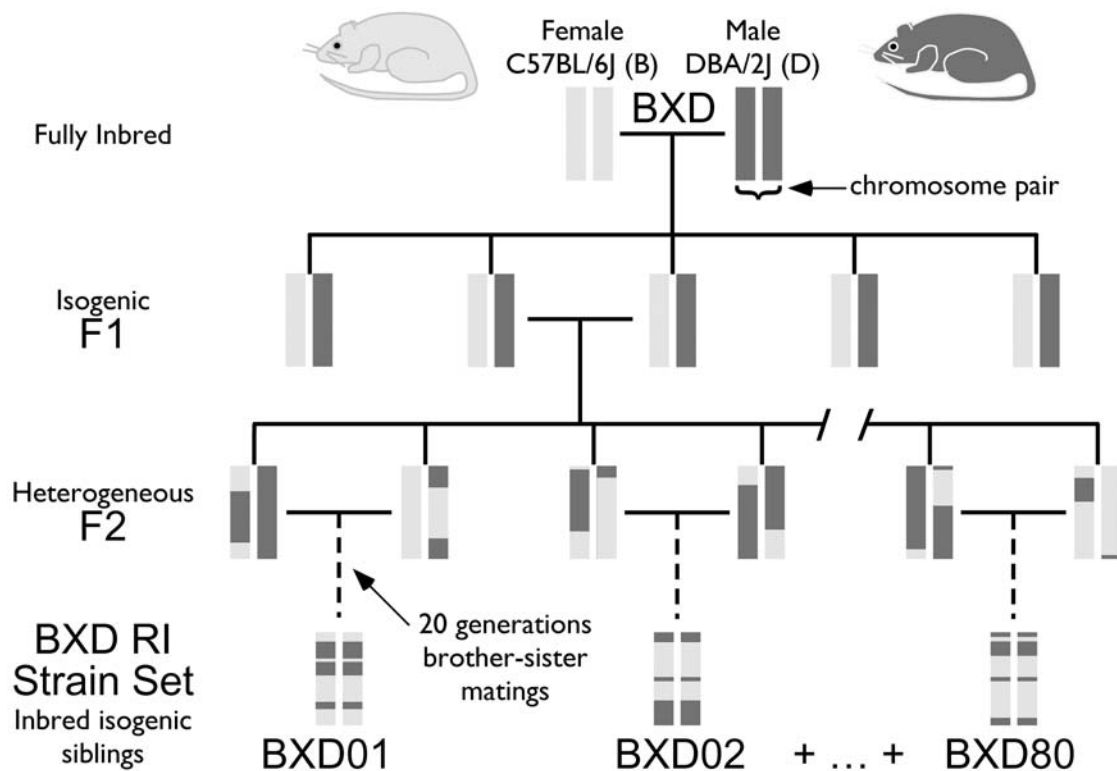


Fig. 2. Illustration of breeding strategy for recombinant inbred (RI) lines. In this example, the generation of the BXD RI set is shown. Parental strains (C57BL/6J and DBA/2J) produce isogenic F1 progeny that are then mated to produce heterogeneous F2 offspring. These F2 animals are then subjected to 20 generations of brother-sister matings, at the end of which, an isogenic inbred strain is created. Multiple pairs of these F2 animals are mated similarly to create multiple BXD lines.

The utility of RI strains for behavioral genetics has been widely recognized (Plomin et al., 1991; Williams et al., 2001a). The strains need to be genotyped only once to generate the marker genotypes used for all subsequent genetic studies. Subsequently, any number of phenotypes can be measured in the RI panel and linked to genotypes. Of almost equal importance, the many different phenotypes can be associated with each other, providing a framework for potentially sophisticated and testable studies of functional correlations. A significant fraction of the shared variance can be explained by specific genetic polymorphisms. Each RI strain can be sampled repeat-

edly and by many investigators over a period of years, allowing more precise measurements of an expanding repertoire of phenotypes—from mRNA abundance, protein levels, and posttranslational modification, through cellular and anatomical correlates, and ultimately extending to behavioral responses to environmental perturbations (Belknap, 1998).

Historically, the main problem in using RI strains to map complex traits has been their limited numbers. The largest set has been a group of 34 BXD strains. The small size of RI sets is a problem that we and others have begun to solve by generating much larger RI sets. The BXD set is now in the process of being expand-

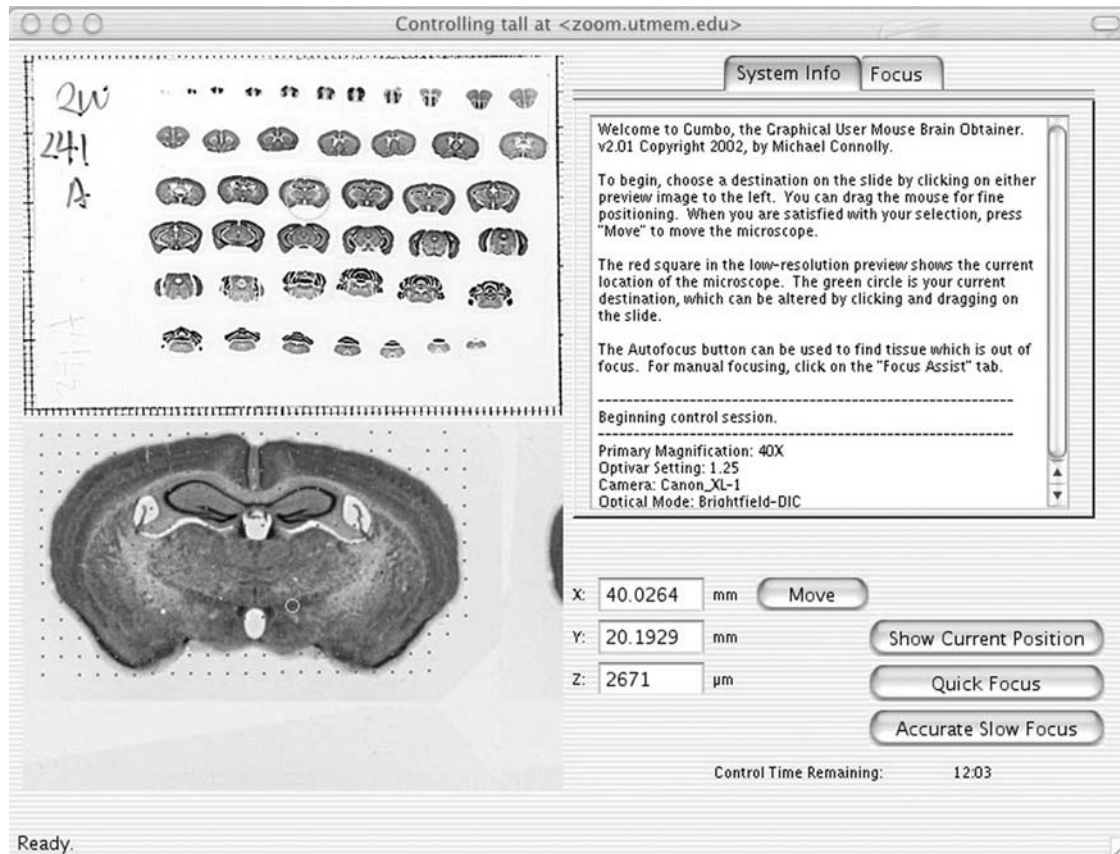


Fig. 3. A screenshot demonstrating the interface of the user interface of the iScope. The user interface is divided into four quadrants. The upper left quadrant contains a thumbnail image of the slide currently being imaged. The bottom left quadrant shows the live image. Interface and focus controls are located on the right.

ed to a total of about 80 lines, which will allow much finer mapping specificity. This enlarged BXD strain set will be of particular interest because they originated from two strains, both of which have been fully sequenced: C57BL/6J and DBA/2J. This means that the ultimate discovery of the relevant allelic variants that are the sources of architectural and behavioral differences among mice will be much easier to define. These new strains will be represented in the MBL as they are generated.

### **The iScope ([iscope.mbl.org](http://iscope.mbl.org))**

The MBL provides access to thousands of

images of histologically processed brains that are ideal for stereologic analysis of regional volume, such as that of the hippocampus, striatum, or cerebral cortex. However, these low-magnification images are not suitable for the analysis of cell number, cell density, or distribution of cell types within these regions of interest. To facilitate stereological analysis by users, we have created the iScope (internet microscope). In short, the iScope provides high resolution, high magnification access to the slides of the MBL over the world-wide-web. We have provided the tools so that users can gain access to these slides either in real-time

by directly controlling a microscope, or offline by directing the microscope to scan specified regions of individual slides, acquire images of these regions, and send these images back to the users.

All access to the iScope occurs through "Gumbo" (Graphical User Mouse Brain Obtainer), our free downloadable control software (available for Windows, Mac OS X, and Linux), which allows users to control their choice from a group of research-grade light microscopes and explore a wealth of mouse tissue at an image resolution of slightly better than  $0.5 \mu\text{m}$ .<sup>1</sup> The iScope consists of three modified upright Zeiss Universal microscopes, nicknamed "Tall," "Dark," and "Handsome." Two are equipped with  $40\times$  achromatic differential interference contrast (DIC) objectives.<sup>2</sup> The third iScope is currently implemented as a  $10\times$  conventional light microscope. Fields are imaged using digital cameras (Sony IIEE1394 digital cameras with  $1280\times 960$  resolution). Each microscope has been modified to accept a motorized x-y stage and z-axis controller, which is interfaced with a controlling Linux computer. The Linux computer integrates the functions

of microscope control, image capture, and web communication with the distant users, who access the system with a custom downloadable application. Together, these systems allow the user to control scheduling, image capture, the interface between previously archived images and real-time ones, the remote control of microscope stages, focus,<sup>3</sup> and, when development is complete, the robotic slide handler.

The interface for the iScope (Fig. 3) allows the user to receive instantaneous feedback as to where on a slide the microscope is focused.

A low power image of the entire  $75\times 50\text{-mm}$  glass microscope slide is presented in a window and moving cursors are superimposed on that image, indicating the present location of the microscope stage. Below this image is a moving higher-power image representing the  $1\text{-cm}$  square of the slide immediately under the objective. It is magnified enough so that nuclear boundaries are easily seen. These two images are from the MBL, and one of the challenges in developing the iScope system was developing a coordinate system that mapped location on the MBL images with x-, y-coordinates of the physical microscope stage being controlled.

---

<sup>1</sup> This resolution is the precisely calibrated value delivered by the optics of the  $40\times$  Zeiss objective and is the highest resolution in the current iScope configuration. All of the details of the optics and pixel resolution of each iScope are presented to the user as a scrollable text file during the sign-on process prior to beginning to control a microscope.

<sup>2</sup> Standard brightfield microscopy of Nissl-stained specimens primarily conveys information about the optical density of the stain, whereas DIC optics reveals differences in the refractive properties of the tissue. DIC optics of stained tissue is thus a multimodal imaging method and as such, provides more information about the tissue than simple brightfield microscopy (Farkas et al., 1993). A number of other advantages of DIC microscopy have been enumerated elsewhere (Williams and Rakic, 1988), including the unique modulation transfer function of DIC images (Inoué and Walter, 1986) and the shallow depth of field. DIC can be thought of as a pseudo-confocal system in which the out-of-focus blur from tissue above and below the focal plane is significantly attenuated (Oldenbourg et al., 1993). It is still not perfect, and many of the problems in high-resolution reconstruction of single cells discussed by Hibbard et al. (1996) remain.

<sup>3</sup> Regarding focus, the user does have control of the z-axis and could conceivably focus through the depth range allowed by the microscope stage hardware until the tissue was found. Manual or user-mediated focusing, however, is impractical due to the  $10\text{--}20\text{ s}$  it takes to capture and transmit an image to the user. The sensible alternative is for the user to invoke our fast and effective server-side automatic focusing mechanism, which involves no transmission of intermediate images over the internet.

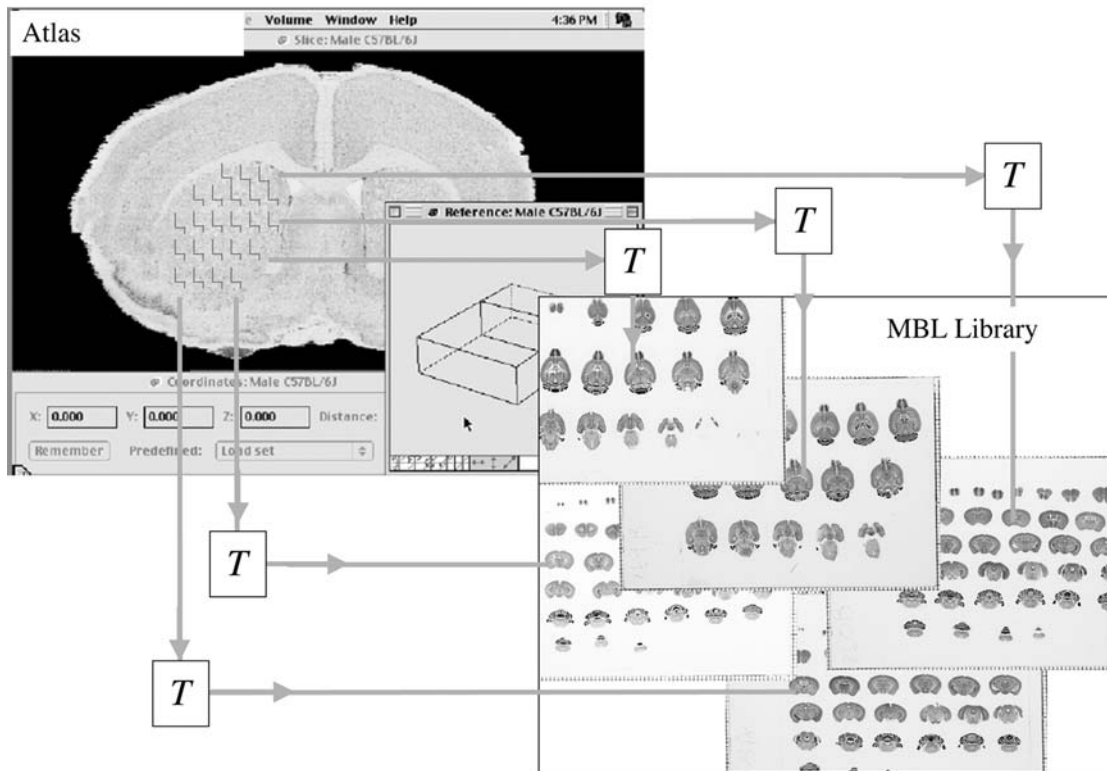


Fig. 4. Atlas-guided navigation. NeuroTerrain, a 3D atlas (upper left panel) is used as an indexer of MBL slides, a number of which are shown in the lower panel). Transformation parameters ( $T$ ) that relate positions on the atlas and corresponding ones on each slide in MBL are determined by registering each MBL slide to the atlas. Using the atlas, a user will be able to define a high-resolution acquisition sampling protocol (illustrated here are count boxes in the caudate nucleus) that will automatically engage the Internet-enabled microscope and robotic slide feeder to obtain the images.

Having gained control of the microscope, the user can then use the iScope to perform stereologic estimates of cell number in real-time, or can request that the iScope capture a through-focus movie of the field for subsequent analysis (see e.g., [http://mbl.org/movies/lgn\\_movies/lgn\\_cells.mov](http://mbl.org/movies/lgn_movies/lgn_cells.mov)).

As mentioned previously, the iScope also provides the ability for the user to request the offline capture of a series of through-focus movies representing a particular region. For example, one could request that the iScope sample 10 sampling sites in each of seven different sections of the striatum and the iScope will go about capturing those movies during

times when it is not otherwise engaged. Using the same system, we have used the iScope to automatically capture through-focus movies of the MBL at 400 brain locations, and have archived these on the website. Thus, rather than having one specify exactly where the iScope should grab images, one can order previously captured images representing the regions of interest.

Along with the project's computer programs, researchers may obtain free stereology software that allows viewers to examine a region of tissue through a light microscope and to record attributes of the region, usually the number, kind, or size of individual cells in the



tissue. While our own emphasis is on probing the complex genetic and environmental basis of variation in CNS architecture, the microscope systems that we have developed, and continue to improve, also have widespread applicability in other research and teaching programs, especially those interested in behavioral research and the brain.

### **Neurocartographer** ([www.neuroterrain.org](http://www.neuroterrain.org))

To be widely useful, easy access is required to the massive physical slide library described previously. The slide collection contains tissue cut at various orientations and the locations of sections on the slide are, of course, not standardized. At the same time, the moderate resolution digital images contained in the database are of insufficient magnification to support cell counting, one of the greatest utilities offered by MBL. Instead, on-demand acquisition at higher resolution is required and will necessitate proper positioning of the sections under the iScope. The objective of this part of our effort is to develop an image-based retrieval system. The approach undertaken is familiar in its general form to those employed elsewhere.

A now common tactic in spatial neuroinformatics calls for a reference atlas and spatial normalization algorithms to map experimental data into that atlas coordinate system (Toga and Thompson, 1999; Baldock et al., 2003; MacKenzie-Graham et al., 2003; Martone et al., 2003). This approach is most highly developed in human neuroimaging. Atlases based on individuals (Talairach and Tournoux, 1988) and populations (Mazziotta et al., 2001a; Mazziotta et al., 2001b) have been constructed and a large repertoire of registration methods developed for PET and MRI data (Toga, 1999).

We have adopted a similar approach. The unique element here is that the atlas is providing access to the physical slides rather than digital data. From the perspective of a user of

MBL, selection of volumes-of-interest (VOIs) on the atlas will direct automated acquisition of high-resolution microscopic samples from the user-selected MBL slides. Our task is to target image collection as depicted in Fig. 4.

Two elements of the retrieval system are of primary importance to the user: a 3D atlas and atlas navigation software. It is these that the user manipulates to direct acquisition. We describe these first before providing a peek under the hood at how the mapping between atlas and library is established.

The front-end to the database is a 3D navigation software package called MacOStat (Gustafson et al., in press). It is available as both a stand-alone application for MacOS and as a lightweight multi-platform Java client. It can display user-selected planes of view through NeuroTerrain, a 3D atlas of the mouse brain. Using straightforward navigation tools, the operator can translate or rotate a virtual knife to reveal arbitrary planes of view (Fig. 5).

In addition to the intensity data, delineated VOIs can be displayed. The atlas itself was constructed from a single adult male C57BL/6J brain. Consecutive 18  $\mu\text{m}$  horizontal sections collected using a low-distortion cryosectioning method (Nissanov et al., 2001) were Nissl stained and reconstructed to yield an 18  $\mu\text{m}$  isotropic dataset.

The atlas and navigation software are freely available from our website. The current version under development will provide support for retrieval of aligned MBL slides and control of the MBL microscopes. The transformations between atlas and slide collection rely on the moderate resolution digital images that are being acquired as new slides are added to the library. In the next software release, the user will be able to view locations where high-resolution acquisitions were obtained overlaid on the moderate resolution images. We will enable selection by users of the desired strains to be imaged and, on the atlas, the VOIs. The atlas will then direct the iScope to collect unbiased

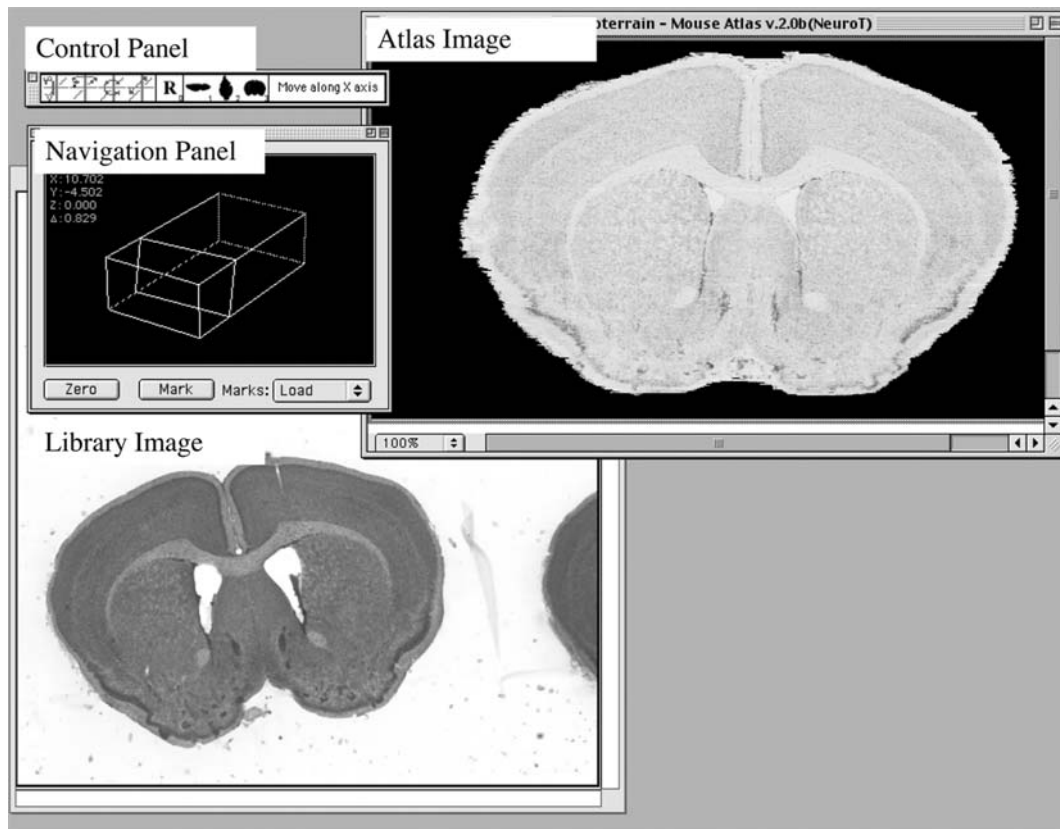


Fig. 5. Atlas navigation and section matching. MacOStat, the atlas navigation software, provides intuitive controls for selection of a plane of view through NeuroTerrain. The view (labeled "Atlas Image") can be selected by dragging the mouse across the navigation window ("Navigation" Panel). The virtual knife motion performed by this interaction depends on selection of an action button from the Control Panel. One can rotate the knife about any of the axes or translate perpendicular to the view presented. Visual matching of an MBL section (Library Image) to the atlas requires navigating to the equivalent plane on the atlas and transferring the plane information to the image.

3D systematic samples in an unsupervised manner. Once complete, the user will be notified of the availability of those datasets and provided with a map of the locations where data was collected. One would then select those collection sites that truly lie within the VOI. Thus, registration error would be overcome by visual inspection. While it is critical to assure that during acquisition the region is properly sampled, a degree of false positives (samples outside the VOI) can be tolerated. We want, however, to limit such oversampling because of the time consuming nature of acquisition

and visual inspection. The problem then is one of how to improve efficiency.

Reduction of oversampling is achieved by registering MBL section images to the atlas. By maintaining information about the position of sections on the physical slide, we can determine the mapping parameters that take one from a location on the atlas to the corresponding position on any of the MBL sections. This registration is performed in-house with the result made available to the MBL navigation system.

Assume, for a moment, that no targeting guidance was available. The entire slide would

then need to be sampled. A tremendous improvement in efficiency is achieved if the locations of the sections on the slide are known and the background excluded from sampling. This is achieved with a texture parcellator that separates the empty background from tissue sections. A further increase in efficiency can be achieved by identifying the likely sections containing the VOI. This can be done automatically (Kozinska et al., 1997; Cohen et al., 1998), though our present preferred approach is manual, as illustrated in Fig. 5. Using MacOStat, the operator can simply navigate through the atlas until a matching view is obtained—the atlas plane coordinates can then be associated with the library image. One need not align each section individually. One can instead align blocks of tissue by matching the first and last section of the tissue span to the atlas and interpolate intermediate positions. For an experienced operator, it takes a few minutes to align each section.

The next step in improving efficiency is alignment of the selected library section to the corresponding atlas plane. We have developed a distance-based algorithm (Kozinska et al., 1997) that is robust in the presence of tissue tears and that relies on the external section contour to guide registration. Under the framework of affine transformation (translation, rotation, magnification, and shear), one can achieve a registration accuracy of 56  $\mu\text{m}$  (as measured by residual mean distance between corresponding anatomical contours; Gefen et al., in press): corresponding positions across brains are aligned on average to within this distance. Following alignment, sampling coordinates within the atlas VOI can be mapped onto the slide to target acquisition.

Improvement over this registration approach can be achieved using nonlinear procedures. We have developed a wavelet-based method that registers sections to within 23  $\mu\text{m}$  (Gefen et al., in press). A difficulty with this

approach is the need for internal landmarks along with the external contour to guide the alignment process. We are employing a range of techniques to obtain these. For example, a path search method (Waks and Tretiak, 1990a,b; Nissanov and McEachron, 1991) is proving useful in locating a large number of anatomical structures. Histogram-based methods are effective in finding key features such as cell layers in the cerebellum and hippocampus. Our major efforts at this point are to construct a neuroanatomic expert system that employs the known plane of view, determined as shown in Fig. 5, to define the appropriate image processing routines to deploy.

Taken together, these steps significantly improve acquisition efficiency. Our overall objective is to achieve targeting accuracy of at least 25  $\mu\text{m}$  for any brain location from any mouse strain. With this level of accuracy, sampling a spherical structure with a 200  $\mu\text{m}$  radius will require sampling a circumscribed volume approx 50% larger. Compared to collecting 3D samples across the two slides containing the sections of a single brain, this corresponds to a nearly 5000-fold improvement in efficiency.

### **WebQTL**

The analysis of complex traits begins with a search for statistical association between trait values of progeny of a cross and the genotypes of those progeny at known marker loci. The goal is a statistical model that predicts a significant fraction of the trait variance. The locations of the markers in a statistically significant model define regions in which genes controlling the trait can be expected. There are a variety of tools that one can use to map quantitative traits, and the reader is referred to <http://mapmgr.roswellpark.org/qtsoftware.html> for a list of commercial and freely distributed programs. We have integrated WebQTL, a web-based QTL mapping program into our collaborative effort. A complete description of this website is

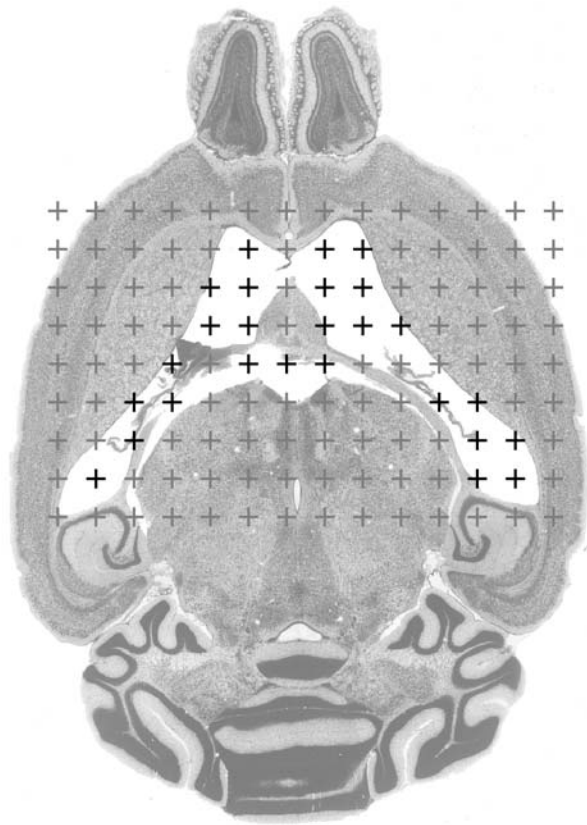


Fig. 6. Illustration of the principles of the point counting procedure for estimating ventricular volume. A grid ( $0.5 \times 0.5$  mm in this example) is overlaid on top of the image, and those points of intersection that fall within the ventricles are counted (red crosses). In this subject, there are 27 points within the ventricles, yielding a surface area measurement of  $13.5 \text{ mm}^2$ . Estimates of ventricular volume are computed using Cavalieri's rule from measures of the surface area from systematically sampled serial sections (Gundersen and Jensen, 1987).

described elsewhere in this issue (Wang et al., 2003). As with all mapping programs, WebQTL will search for QTLs, but it is designed specifically to support shared mapping populations—five sets of mouse RI lines and one advanced intercross. That is, WebQTL will search for QTLs using traits measured in the CXB, AXB, BXA, BXD, or BXH sets<sup>4</sup> of mouse RI lines (the advantages of RI lines are discussed previously). Moreover, WebQTL

includes integrated databases with both genotype and quantitative trait data for the supported RI lines, particularly the BXD set. Finally, WebQTL will search for correlations between a selected or user-defined trait and traits in one of its databases. This feature is especially useful for finding correlations between biological traits and expression of particular genes as assayed by microarray hybridization (Chesler et al., this issue).

### QTLs for Cerebral Ventricle Size: A Practical Example

As a means of illustrating the usefulness of the MBL, we will briefly present a recent investigation that exploited the tools described previously (Zygourakis and Rosen, 2003). Using stereologic techniques, we estimated cerebral ventricle size in a total of 228 AXB and BXA RI strains and their parental strains (A/J and C57BL/6J). This set is particularly appropriate because A/J have small ventricles, whereas C57BL/6J have large ventricles. We calculated brain and cerebral ventricle volumes from MBL images using point counting with NIH Image (see Fig. 6).

The morphometric data were analyzed using ANOVA and multiple regression techniques, and QTL analysis was carried out with QTX (Manly et al., 2001) and WebQTL.

We computed a heritability factor ( $h^2$ ) of 0.32 for ventricular size, which is about on par with other anatomic phenotypes. We regressed ventricle volume for each of the RI subjects against age, sex, plane of section, brain weight, and histologic brain volume and mapped the rank order of these residuals. We found a significant QTL on Chr 8, between markers *D8Mit94* and *D8Mit189* (LOD=4.3, genome-wide  $p < 0.05$ ), and suggestive QTLs on Chrs 4, 7, and 12 (see Fig. 7).

<sup>4</sup> "A" = A/J; "B" = C57BL/6J; "D" = DBA/2J; "H" = C3H.

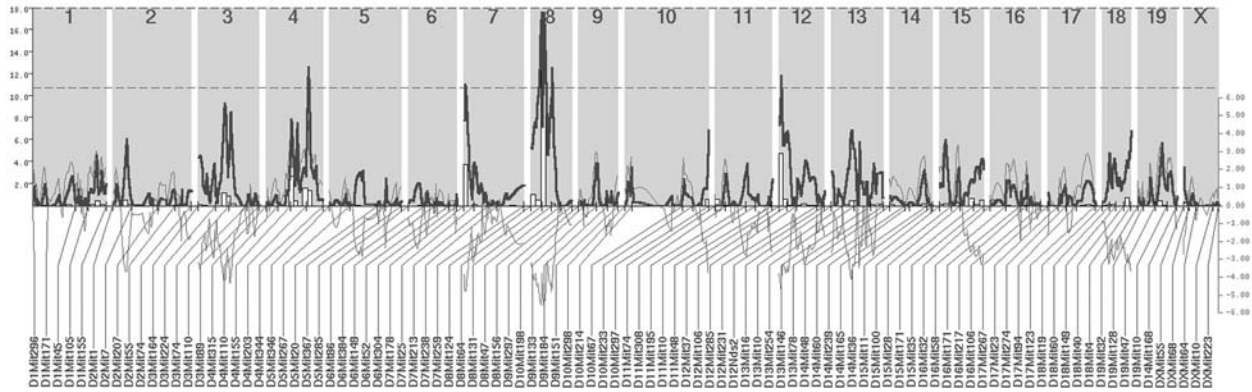


Fig. 7. Genome-wide interval mapping of cerebral ventricle size in AXB, BXA RI mice. The solid line represents the likelihood ratio statistic as determined by marker regression at each of the microsatellite markers along the x-axis. The gray histogram represents the results of the bootstrap analysis, and shows that the overwhelming majority of the 1000 permutations in this analysis aligned within the QTL interval defined by the marker regression. Dotted line is the additive effect—a negative number indicates the trait is modulated by the “B” allele. LRS scores are equal to 4.6 times the LOD score.

Subjects with an allele from the C57BL/6J parent (“B”) parent had significantly larger ventricles than those with an allele from the A/J (“A”) parent. We also found a highly significant interactive allele between markers on Chrs 4 and 7 (LRS = 45.1,  $p < 0.001$ )—subjects with B alleles at each marker had significantly larger ventricles than those subjects with only one B allele. Interestingly, these QTLs are in close proximity to genes associated with hydrocephalus in mice, including *Tgfb1* on Chr 7 and *Tgfb1r* on Chr 4 (Galbreath et al., 1995; Wyss-Coray et al., 1995; Hayashi et al., 2000; Moinuddin and Tada, 2000). The important point to emphasize for the current discussion is that these data were gathered using solely the resources available on the MBL.

## Conclusions

To begin to understand the design of the brain, whether that of a mouse or a human, we need to extract the key genes that control and modulate cell proliferation, differentiation, and

survival. A significant fraction of genes are polymorphic—that is, they exist in multiple forms or alleles—and differences in alleles generate variation in CNS structure that may be subtle or quite extreme. Normal variation is a significant source of the fascinating and sometimes disturbing behavioral differences among humans. Only by combining efforts can scientists efficiently tackle the complex genetics of CNS structure. In the next decade, it is our hope that this Center will revolutionize quantitative neuroanatomy and stereology and give this field a broad quantitative genetic foundation. The promise of neuroinformatics is to integrate disparate, yet complementary, groups in their search for common understanding of complex data. By genotyping such a large sample of mice and then placing the results on the web together with large collections of “virtual” slides, we hope to free other scientists from the budget and time constraints that would otherwise continue to hamper quantitative neuroanatomic studies. We encourage scientists to use these resources and to share their results

so that the appropriate data on phenotype and genotypes can be added to the expanding database on variation of the mouse CNS.

## Acknowledgments

This work was supported by the Human Brain Project through grant P20 MH62009 funded jointly by NIMH, NIDA, and NSF.

## References

- Airey D. C., Lu L., and Williams R. W. (2001) Genetic control of the mouse cerebellum: Identification of quantitative trait loci modulating size and architecture. *J. Neurosci.* 21, 5099–5109.
- Baldock R. A., Bard J. B. L., Burger A., et al. (2003) EMAP and EMAGE: a framework for understanding spatially organized data. *Neuroinformatics* 1, 309–326.
- Belknap J. K. (1998) Effect of within-strain sample size on QTL detection and mapping using recombinant inbred mouse strains. *Behav. Genet.* 28, 29–38.
- Chesler E. J., Wang J., Lu L., Manly K. F., and Williams R. W. (2003) Genetic correlates of gene expression in recombinant inbred strains: a relational model system to explore neurobehavioral phenotypes. *Neuroinformatics* 1, 343–358.
- Cohen F. S., Yang Z., Huang Z., and Nissanov J. (1998) Automatic matching of homologous histological sections. *IEEE Trans. Biomed. Eng.* 45, 642–649.
- Crabbe J. C., Belknap J. K., Mitchell S. R., and Crawshaw L. I. (1994) Quantitative trait loci mapping of genes that influence the sensitivity and tolerance to ethanol-induced hypothermia in BXD recombinant inbred mice. *J. Pharmacol. Exp. Ther.* 269, 184–192.
- Curcio C. A. and Allen K. A. (1990) Topography of ganglion cells in human retina. *J. Comp. Neurol.* 300, 5–25.
- Farkas D. L., Baxter G., DeBiasio R. L., et al. (1993) Multimode light microscopy and the dynamics of molecules, cells, and tissues. *Annu. Rev. Physiol.* 55, 785–817.
- Galbreath E., Kim S. J., Park K., Brenner M., and Messing A. (1995) Overexpression of TGF-beta 1 in the central nervous system of transgenic mice results in hydrocephalus. *J. Neuropathol. Exp. Neurol.* 54, 339–349.
- Gefen S., Tretiak O., Bertrand L., Rosen G., and Nissanov J. Surface alignment of an elastic body using a multi-resolution wavelet representation. *IEEE Trans Biomed Eng.*, in press.
- Gilissen E. and Zilles K. (1996) The calcarine sulcus as an estimate of the total volume of human striate cortex: a morphometric study of reliability and intersubject variability. *J. Hirnforsch.* 37, 57–66.
- Gilissen E. and Williams R. W. (1997) Genetic dissection and QTL analysis of forebrain, hindbrain, olfactory bulb, and cerebellum. *Society for Neuroscience Abstracts* 23, 864.
- Gundersen H. J. G. and Jensen E. B. (1987) The efficiency of systematic sampling in stereology and its prediction. *J. Microscop.* 147, 229–263.
- Gustafson C., Tretiak O., Bertrand L. and Nissanov J. Design and implementation of software for assembly and browsing of 3D brain atlases. *Comput Methods Programs Biomed.*, in press.
- Hayashi N., Leifer D. W., and Cohen A. R. (2000) Chronologic changes of cerebral ventricular size in a transgenic model of hydrocephalus. *Pediatr. Neurosurg.* 33, 182–187.
- Hibbard L. S., McCasland J. S., Brunstrom J. E., and Pearlman A. L. (1996) Automated recognition and mapping of immunolabelled neurons in the developing brain. *J. Microsc.* 183 (Pt 3), 241–256.
- Horton J. C. and Hocking D. R. (1996) Intrinsic variability of ocular dominance column periodicity in normal macaque monkeys. *J. Neurosci.* 16, 7228–7239.
- Inoué S. and Spring K. R. Video microscopy—the Fundamentals. 1997, Plenum, New York.
- Johnson T. E., Defries J. C., and Markel P. D. (1992) Mapping quantitative trait loci for behavioral traits in the mouse. *Behav. Genet.* 22, 635–653.
- Kanes S., Dains K., Cipp L., et al. (1996) Mapping the genes for haloperidol-induced catalepsy. *J. Pharmacol. Exp. Ther.* 277, 1016–1025.
- Kozinska D., Tretiak O., Nissanov J., and Ozturk C. (1997) Multidimensional alignment using the Euclidean distance transform. *Graphical Models and Image Processing* 59, 373–387.
- Lander E. S. and Schork N. J. (1994) Genetic dissection of complex traits. *Science* 265, 2037–2048.
- Lipp H. P., Schwegler H., Crusio W. E., et al. (1989) Using genetically-defined rodent strains for the identification of hippocampal traits relevant for two-way avoidance behavior: a non-invasive approach. *Experientia* 45, 845–859.
- Lu L., Airey D. C., and Williams R. W. (2001) Complex trait analysis of the hippocampus: map-

- ping and biometric analysis of two novel gene loci with specific effects on hippocampal structure in mice. *J. Neurosci.* 21, 3503–3514.
- MacKenzie-Graham A., Jones E. S., Shattuck D. W., Dinov I., Bota M., and Toga A. W. (2003) The informatics of a C57BL/6 Mouse Brain Atlas. *Neuroinformatics* 1, 397–410.
- Manly K. F., Cudmore R. H. J., and Meer J. M. (2001) Map Manager QTX, cross-platform software for genetic mapping. *Mammalian Genome* 12, 930–932.
- Martone M. E., Zhang S., Gupta A., et al. (2003) The cell-centered database: a database for multiscale structural and protein localization data from light and electron microscopy. *Neuroinformatics* 1, 379–396
- Mazziotta J., Toga A., Evans A., et al. (2001a) A probabilistic atlas and reference system for the human brain: International Consortium for Brain Mapping (ICBM). *Philos. Trans. R. Soc. Lond. B. Biol. Sci.* 356, 1293–1322.
- Mazziotta J., Toga A., Evans A., et al. (2001b) A four-dimensional probabilistic atlas of the human brain. *J. Am. Med. Inform. Assoc.* 8, 401–430.
- Moinuddin S. M. and Tada T. (2000) Study of cerebrospinal fluid flow dynamics in TGF-beta 1 induced chronic hydrocephalic mice. *Neurol. Res.* 22, 215–222.
- Nissanov J. and McEachron D. L. (1991) Advances in image processing for autoradiography. *J. Chem. Neuroanat.* 4, 329–342.
- Nissanov J., Bertrand L., and Tretiak O. (2001) Cryosectioning distortion reduction using tape support. *Microsc. Res. Tech.* 53, 239–240.
- Oldenbourg R., Terada H., Tiberio R., and Inoue S. (1993) Image sharpness and contrast transfer in coherent confocal microscopy. *J. Microsc.* 172 (Pt 1), 31–39.
- Pakkenberg B. and Gundersen H. J. (1997) Neocortical neuron number in humans: effect of sex and age. *J. Comp. Neurol.* 384, 312–320.
- Plomin R., McClearn G. E., Gora-Maslak G., and Neiderhiser J. M. (1991) Use of recombinant inbred strains to detect quantitative trait loci associated with behavior. *Behav. Genet.* 21, 99–116.
- Rosen G. D. and Williams R. W. (2001) Complex trait analysis of the mouse striatum: Independent QTLs modulate volume and neuron number. *BMC Neuroscience.* 2, 5.
- Stensaas S. S., Eddington D. K., and Dobelle W. H. (1974) The topography and variability of the primary visual cortex in man. *J. Neurosurg.* 40, 747–755.
- Takahashi J. S., Pinto L. H., and Vitaterna M. H. (1994) Forward and reverse genetic approaches to behavior in the mouse. *Science* 264, 1724–1733.
- Talairach J. and Tournoux P. (1988) *Co-Planar Stereotaxic Atlas of the Human Brain*, 1st ed., Thieme Medical Publishers, Inc., New York.
- Toga A. W., ed. (1999) *Brain Warping*, Academic Press, New York.
- Toga A. W. and Thompson P. M. (1999) An Introduction to Brain Warping, in *Brain Warping* (Toga A. W., ed), pp. 1–26. Academic Press, New York.
- Waks A. and Tretiak O. J. (1990a) Recognition of regions in brain sections. *Computerized Medical Imaging and Graphics* 14, 341–352.
- Waks A. and Tretiak O. J. (1990b) Image segmentation through robust edge detection. In: *IEEE International Conference on Robust Computer Vision*, Washington DC, pp. 302–324.
- Wang J., Williams R. W., and Manly K. F. (2003) WebQTL: Web-based complex trait analysis. *Neuroinformatics* 1, 299–308.
- Williams R. W. (2000) Mapping genes that modulate mouse brain development: A quantitative genetic approach, in *Mouse Brain Development* (Goffinet A. and Rakic P., eds), Springer, Berlin, pp. 21–49.
- Williams R. W. and Rakic P. (1988) Three-dimensional counting: An accurate and direct method to estimate numbers of cells in sectioned material. *J. Comp. Neurol.* 278, 344–352.
- Williams R. W. and Herrup K. (1988) The control of neuron number. *Annu. Rev. Neurosci.* 11, 423–453.
- Williams R. W., Cavada C., and Reinoso-Suarez F. (1993) Rapid evolution of the visual system: a cellular assay of the retina and dorsal lateral geniculate nucleus of the Spanish wildcat and the domestic cat. *J. Neurosci.* 13, 208–228.
- Williams R. W., Strom R. C., and Goldowitz D. (1998) Natural variation in neuron number in mice is linked to a major quantitative trait locus on Chr 11. *J. Neurosci.* 18, 138–146.
- Williams R. W., Strom R. C., Rice D. S., and Goldowitz D. (1996) Genetic and environmental control of variation in retinal ganglion cell number in mice. *J. Neurosci.* 16, 7193–7205.
- Williams R. W., Gu J., Qi S., and Lu L. (2001a) The genetic structure of recombinant inbred mice: high-resolution consensus maps for complex trait analysis. *Genome Biol.* 2, 0046.
- Williams R. W., Lu L., Kulkarnik A., Zhou G., and Airey D. C. (2001b) Genetic dissection of the olfac-

- tory bulbs of mice: QTLs on chromosomes 4, 6, 11, and 17 modulate bulb size. *Behav. Genet.* 31, 61–77.
- Wyss-Coray T., Feng L., Masliah E., et al. (1995) Increased central nervous system production of extracellular matrix components and development of hydrocephalus in transgenic mice over-expressing transforming growth factor-beta 1. *Am. J. Pathol.* 147, 53–67.
- Zygourakis C. C. and Rosen G. D. (2003) Quantitative trait loci modulate ventricular size in the mouse brain. *J. Comp. Neurol.* 461, 362–369.